Oxygen as a primary selective pressure for photo-endosymbiosis evolution

Loïc Quevarec[1-2], Rachel Bonnarde[1-2], Christophe Robaglia[1*], Gaël Brasseur[2*]

[1]Aix Marseille Université, CEA, CNRS, BIAM, Luminy Génétique et Biophysique des Plantes, 13009 Marseille, France

[2]Laboratoire de Chimie Bactérienne, IMM, CNRS, Aix-Marseille Université, 13402 Marseille, France

*Co-corresponding authors: christophe.robaglia@univ-amu.fr, brasseur@imm.cnrs.fr

Keywords

Tetrahymena thermophila, *Synechoccocus elongatus*, *Chlorella variabilis*, photo-endosymbiosis, evolution, oxygen, carbon, phagocytosis.

Abstract

Photosymbiosis through eukaryotic or eukaryotic – prokaryotic associations provide energy and oxygen to the living world, however the mechanisms behind their evolution remain unknown. Here we develop a naïve system based on the predatory ciliate *Tetrahymena thermophila*, not known for hosting symbiont, to recapitulate early events leading to photosymbiosis evolution. *T. thermophila* was found to readily phagocyte eukaryotic algae (*Chlorella variabilis*) or cyanobacteria (*Synechoccocus elongatus*) that can reach high numbers within predatory cells. Feeding with either prey in a low carbon environment provide little or no growth advantage to *T. thermophila*. In contrast, in anoxic environment, both intracellular *C. variabilis* or *S. elongatus* can readily support growth of *T. thermophila*, in the light but not in the dark, demonstrating that oxygen *in hospite* supply can be an initial feature supporting further photo-

endosymbiosis evolution. This suggests that it is unlikely that carbon metabolites produced by phototrophs could have represented a selective advantage for the evolution of photosymbionts. Although most extant photosymbiosis are based on carbon supply to the host cell, we therefore propose that it is a secondary event occurring from initial evolution in anoxic or hypoxic conditions, where O_2 production was crucial for establishing the initial steps of photosymbiosis.

Introduction

Oxygenic photosynthesis appeared in cyanobacteria probably around 3 Byr ago (Fischer et al., 2016). Using light energy, it provides the chemical energy allowing to fix atmospheric CO_2 into building block of life, supporting the proliferation of photosynthetic organisms and indirectly the organisms that feed on them. Photosynthesis was acquired by eukaryotes by engulfing cyanobacteria, around 1.6 Byr ago (Archibald, 2015; Bhattacharya et al., 2023), leading to the Archaeplastida group, containing the Glaucophyta, the Rhodophyta (red algae) and the Viridiplantae (green algae and land plants) (Ponce-Toledo et al., 2019). Integration of a photosynthetic prokaryote within a eukaryote is known as primary endosymbiosis and have also been described for the amoeba *Paulinella chromatophora* and dated around 90–140 million years ago (Delaye et al., 2016; Ponce-Toledo et al., 2019). Further spreading of photosynthesis occurred by integration of photosynthetic eukaryotes within eukaryotes and are known as secondary and higher order endosymbiosis events. They concern the majority of eukaryotic groups (Lane et Archibald, 2008; Ponce-Toledo et al., 2019). Photosynthetic endosymbiosis is globally present on the entire surface of the Earth and have a considerable impact on environments and the other species that populate them (Bowles et al., 2023).

The recurrent acquisition of photosynthesis by photosymbiosis across the tree of life (Ponce-Toledo et al., 2019), indicates that it is a highly advantageous trait, selected multiple times independently, i.e. convergent evolution (Keeling, 2010). Observable cases of photosymbiosis show that symbionts are initially acquired by predation, particularly by phagocytosis (Gavelis et Gile, 2018; Inouye et Okamoto, 2005; Quevarec et al., 2024). The production of sugars or oxygen by the photosynthetic symbiont and supplied to the host are likely to support the evolution of photosymbiosis (Germond et al., 2013). Extant stable photosymbiosis in plants and algae are clearly based on carbon autotrophy (Hoefnagel et al., 1998). A few examples also suggest that the host can benefits from photosynthetically evolved oxygen. Photosymbiotic

ciliates were found particularly abundant at the oxic-anoxic boundary in shallow warm waters, around 2.5 m depth (Finlay et al., 1996). At this depth, there is sufficient light to evolve enough oxygen to support aerobic metabolism. A photosymbiotic ciliate, *Tetrahymena utriculariae*, was discovered in the anoxic traps of the aquatic carnivorous plant *Utricularia reflexa*, where dissolved carbon and other nutrients are abundant (Pitsch et al., 2017). However, most data, if not all, come from already established photosymbiotic associations, where host and symbiont had ample time to co-evolve, therefore the evolutionary trajectories and early events leading to stabilised associations remain unknown.

In this work, using a predator-prey model system, we experimentally evaluate what could be the primary selective force for photosymbiosis establishment. We used the ciliate *T. thermophila* as a model of predatory unicellular host, the cyanobacterium *Synechococcus elongatus* and the eukaryotic green algae *Chlorella variabilis* as preys. Those can recapitulate events leading to either primary (*S. elongatus*) or secondary (*C. variabilis*) endosymbiosis. *T. thermophila* is a widely used model organism, that can grow by osmotrophy or phagocytosis of various prey (Lynn et Doerder, 2012; Wloga et Frankel, 2012). Despite being studied since many years it has never been found to stably host photosynthetic symbionts in the wild. However, related species such as *Paramecium bursaria* (Fujishima et Kodama, 2022) or *T. utricularia* (Pitsch et al., 2017) and many other ciliates are known to host algal symbionts (Johnson, 2011). The freshwater cyanobacterium *S. elongatus* is a well described photosynthetic species (Adomako et al., 2022), living as a possible symbiont within *Crassostrea gigas* tissues (Avila-Poveda et al., 2014). The *Synechococcus* genus has the greatest genetic proximity to the *P. chromatophora* chromatophore which result from a recent primary endosymbiosis (Delaye et al., 2016; Nowack et al., 2008; Ponce-Toledo et al., 2019). *C. variabilis* is a well described photosynthetic algal species (Krienitz et al., 2015), which, together with others members of its genus, are symbiont in many endosymbiosis (i.e. with *P.*

bursaria (Zagata et al., 2016), *Hydra viridissima* (Rajević et al., 2015), *Stentor pyriformis* (Hoshina et al., 2021) or *Acanthocystis turfacea* (Matzke et al., 1990)).

We show that in an initial predatory-prey state the supply of carbon by photosynthetic prey support modestly the growth of the predator, while the supply of oxygen leads to a readily observable growth advantage, making it a likely proximal selective pressure for initiation of photo-endosymbiosis.

Results

Phagocytosis dynamics

In coculture with the cyanobacterium *S. elongatus* UTEX 2973, *T. thermophila* phagosomes containing several red autofluorescent bacteria were readily observed (Fig. 1F). Flow cytometry using both scatter density and chlorophyll-fluorescence was further used to quantify the rate and the amplitude of the phagocytosis process. This experiment showed a fast period of bacterial phagocytosis leading to a maximum of 160 cyanobacteria accumulated per *Tetrahymena* cells at a calculated maximum initial speed of about 800 cyanobacteria phagocyted per hour (1 cyanobacteria phagocyted every 4.5 s) (Fig 2). This period is followed by a longer period during which cyanobacterial cells progressively disappeared at a rate of about 20 cyanobacteria per hour (Fig S2B). This kind of phagocytic behaviour was previously reported for *Tetrahymena pyriformis* (Thurman et al. 2010). We noticed that around 40 min after the initiation of coculture, a new population of fluorescent particles appears with an intermediate size between *T. thermophila* and *S. elongatus*. Fluorescent microscopy shows that they were often localized at the cytoproct and were likely droppings (faecal pellets) ejected by *Tetrahymena* and containing up to 4 cyanobacterial cells (Fig. 2C, D and Fig. 2G for droppings image).

In a coculture between *T. thermophila* and *C. variabilis* a first rapid phase of phagocytosis at a maximum rate of about 40 algae phagocyted per hour (1 every 1.6 min) succeeded a slower phase were *C. variabilis* cells progressively disappeared at a rate of 3.7 cells per hour (Fig. 3A and B). The uptake of up to 40 algal cells per *T. thermophila* cell was monitored (Fig. 3B, Fig. S3). The average size of free *C. variabilis* cells increased during the phagocytosis process, suggesting a selective preference by *T. thermophila* possibly linked to the size of its oral apparatus (6-10 µM) compared to that of *C. variabilis* cells (3-10 µM) (Fig. S3b).

In a coculture with a GFP labelled *Escherichia coli* - bacterium, up to 700 bacterial cells were phagocyted in one hour with a maximum initial rate at the onset of more than 3000 *E. coli*/hour (Fig. S4B – D). After one hour of phagocytosis, droppings containing up to 7 *E. coli* appeared (Fig. S4A and E).

Coculture with both *E. coli*-GFP and *C. variabilis* showed that both type of cells could be simultaneously ingested. *E. coli* phagocytosis was found markedly faster than that of *C. variabilis,* possibly linked to its smaller size (data not shown).

Carbon benefit for *T. thermophila* through phagocytosis of phototrophs

We tested the contribution of carbon (sugars) produced by photosynthetic preys on the growth of *T. thermophila. T. thermophila* grew significantly in the rich Neff medium with *S. elongatus* (Fig. 4A; Table S1C) or *C. variabilis* (Fig. 4B; Table S2C) or without phototrophs compared with a culture of *T. thermophila* in mineral minimum TAP medium (Fig. 4A and B; Table S1C and S2C). In this rich Neff medium, the presence of phototrophs did not increase the growth yield and rate of *T. thermophila* (Table S1C and S2C, Fig. 4A and B). In the mineral minimum TAP medium, no growth of *T. thermophila* alone was observed even with the addition of *C. variabilis* (Table S2C; Fig. 4B). However, adding *S. elongatus* increased slightly the growth of *T. thermophila* (Table S1C; Fig. 4A).

In the modified PP medium (Fig. 4C – E), the growth of *T. thermophila* is stimulated in the presence of *S. elongatus* in the light but not in the dark (Table S3A; Fig. 4C). With *C. variabilis*, a significant decrease in the growth of *T. thermophila* both in the light and in the dark was observed compared with a culture of *T. thermophila* alone (Table S4A; Fig. 4D). The non-photosynthetic *E. coli* significantly fuelled the growth of *T. thermophila* PP medium (Table S5A; Fig. 4E), although this growth is still less efficient than *T. thermophila* alone in the rich Neff medium (Fig. 4A).

Oxygen benefit for *T. thermophila* through phagocytosis of phototrophs

We probed the lower limit of oxygen concentration to allow *T. thermophila* growth (Fig. 5A). Optimum growth occurs at atmospheric tension of 21% O_2, while significant growth occurs with as little as 0.05% oxygen compared with a totally anoxic environment (Fig. 5A; Table S6). We then initiate anoxic cocultures in conditions where most phototrophs were found to be phagocyted within a short period of time, as defined both by flow cytometry and confirmed by fluorescent microscopy. In the dark and anaerobic conditions, *T. thermophila* did not grow and even lysed in the presence of all kind of preys (Fig. 5B and C). In contrast phagocyted phototrophs efficiently support *T. thermophila* growth in anoxia significantly in the light but not in the dark. In anoxic co-culture with the non-phototrophic *E. coli*, *T. thermophila* did not grow either the light or in dark (Fig. 5D).

These experiments strongly suggest that oxygen evolved by phagocyted photosynthetic preys in the light can rescue *T. thermophila* growth in anoxia. This was further supported in experiments where *T. thermophila* and phototrophs cultures were separated by a tubing and sterile gas filter that only allow gaseous products to diffuse between flasks (not shown).

We next used flow cytometry to evaluate the influence of anoxia on the phagocytosis competence of *T. thermophila*. In anoxia in the dark, *T. thermophila* is unable to phagocyte either *S. elongatus* or *C. variabilis* whereas in anoxia and in the light, the phagocytosis is restored up to more than 100 *S. elongatus* and 9 *C. variabilis* per *T. thermophila* cell. The transit time of ingested photosynthetic cells was found to be reduced in anoxia compared to oxic condition (Fig. 6A and B).

Prey O_2 production and predator O_2 consumption are compatible

We measured O_2 consumption by *S. elongatus*, *C. variabilis* and *T. thermophila* and O_2 production by *S. elongatus* and *C. variabilis* at their maximal rate in presence of saturating amount of substrate (glucose) or light with a modified oxygraph device (Fig. 7; Table 1; Fig. S5). *T. thermophila* mitochondrial O_2 consumption amounts to 43 nmol O_2/min/mg proteins (i.e. 430 x 10^{-16} moles O_2/min/cell) with endogenous substrates present in the cells (Fig. S5B) and to 60 nmol O_2/min/mg (i.e. 600 x 10^{-16} moles O_2/min/cell) using glucose as substrate (Fig. 7; Table 1). This activity is completely inhibited by cyanide, a terminal oxygen reductase inhibitor (Fig. S5B – C). *C. variabilis* and *S. elongatus* exhibits an O_2 consumption activity in the dark of 67 and 20 nmol O_2/min/mg, respectively (Fig. 7 and S5C – D). For O_2 production in the light, *C. variabilis* and *S. elongatus* produce 190 and 105 nmol O_2/min/mg (i.e. around 2.3 and 0.4 x 10^{-16} moles O_2/min/cell) (Table 1; Fig. S5C – D), respectively. This implies that about 260 *C. variabilis*. and 1500 *S. elongatus* per *T. thermophila* cell would be required to provide the equivalent of the atmospheric oxygen concentration (21% O_2), while only a fraction of these numbers would be required to provide the minimal O_2 concentration supporting *T. thermophila* growth (0.05% O_2). After 30 min of phagocytosis, *S. elongatus* included in phagosomes are still able to produce O_2 with light at a similar rate compared to free cyanobacteria (Fig. S5D).

Discussion

Stable photosymbiosis evolved independently in many species of ciliates, including in *Tetrahymena* species (*T. utriculariae*). *T. thermophila* is not known to host photosynthetic symbionts in nature but is able to phagocyte different species of prokaryotic or eukaryotic phototrophs and long-term co-culture with algae and bacteria has been described (Germond et al., 2013; Sano et al., 2009). Assuming that photosymbiosis evolve from predation, this makes *T. thermophila* a suitable evolutionary model to explore the early events that can support a prey to symbiont transition.

Conceptually, from the predator's (host's) point of view, the evolution of a mutualistic symbiosis requires them to benefit from a greater inheritable selective advantage by maintaining prey (symbionts) than by digesting them. Depending on the environment, energetic cost of maintaining the symbiont can be compensated by the byproducts of photosynthesis such as exudated sugars or dioxygen molecule fuelling aerobic nutrient acquisition (from osmotrophy or predation). We wished to test these scenarios using *T. thermophila* as a predator, *C. variabilis* and *S. elongatus* as photosynthetic eukaryotic and prokaryotic preys and *E. coli* as a non-photosynthetic prey.

In co-culture with *T. thermophila*, *E. coli* is rapidly phagocyted and can support growth of *T. thermophila* in a low-carbon media (Fig. 4E). Although fecal pellets containing fluorescent cells can be observed, suggesting incomplete digestion, this show that *E. coli* is fairly susceptible to phagocytosis and digestion by *T. thermophila* (Gurijala et Alexander, 1990; Matsui et al., 2000).

In low carbon media, *T. thermophila* derives a slight growth advantage from the phagocytosis of *S. elongatus* in the dark that is enhanced in the light (Fig. 4C), showing a slight positive effect of photosynthesis that can be due to a better nutrient supply from cyanobacteria cells or by the production of exudates. *S. elongatus* is known to be digested by numerous groups of

predatory unicellular eukaryotes (Christaki et al., 1999; Dillon et Parry, 2009; Dolan et Šimek, 1998), although it is a relatively poor-quality food source (Apple et al., 2011). The amount of exocytosed autofluorescent faecal pellets containin*g* undigested *S. elongatus* cells shows that it is partially resistant to digestion (Fig. 2C), explaining the relatively modest growth advantage provided by comparison to *E. coli*.

In contrast, *T. thermophila* appears unable to benefit from phagocytosis of *C. variabilis*, either by digestion or by the use of exudates (Fig. 4B and D). Indeed, a significant reduction in growth either in the light or in the dark indicates the presence of a cost (Fig. 4D). Species of Chlorella can be established as symbiont in different hosts, including ciliates. They are known to escape from the digestive vacuole into the cytoplasm to form a perialgal vacuole (or symbiosome) (Kodama et Sumita, 2022). Although the precise mechanism is unknown, *Chlorella* sp. could prevent fusion of the lysosome with the phagosome (Karakashian et Rudzinska, 1981) or acquire temporary resistance to lysosomal enzymes (Kodama et al., 2007).

The cost on *T. thermophila* growth by *C. variabilis* can have several causes. Chlorella is not known to release toxins, but a lethal effect of lectins produced by *Chlorella vulgaris* on mosquito *Aedes aegypti* larvae was observed (Cavalcanti et al., 2021). Intracellular accumulation without digestion of *C. variabilis* can inhibit *T. thermophila* growth or cell division. *C. variabilis* is progressively eliminated from *T. thermophila* cytoplasm as faecal pellets.

In sheer contrast to the modest or inexistent benefit provided by phagocyted phototrophs in low carbon media, compared to *E. coli*, growth of *T. thermophila* was significantly stimulated in anoxia in the presence of either *C. variabilis* or *S. elongatus*. This effect was dependent on light, showing that photosynthesis was required. It was observed in conditions where most preys are intracellular (Fig. 5). Quantification of maximum oxygen production and consumption shows that the maximum number of phagocyted preys (40 *C. variabilis* and 160 *S. elongatus* per *T.*

thermophila cell) are fully compatible with *T. thermophila* energy requirements in sub-atmospheric O_2 (Fig. 2, 3 and 7, Table 1).

This demonstrates that predation on photosynthetic cells can provide an immediate growth advantage caused by photosynthetically evolved oxygen in hypoxic environments. This advantage appears more consistent than the provision of sugars (or other carbon compounds) in carbon starved environments.

Evolution towards photosymbiosis can occur through different events such involving evasion from digestion by the prey (Lürling, 2021) or cell retention by the predator/host (Johnson, 2011). *Chlorella* species are known as photosymbionts of many different hosts (Hoshina et al., 2021; Matzke et al., 1990; Rajević et al., 2015; Zagata et al., 2016). *C. variabilis* cells are resistant to digestion by *T. thermophila,* but they slowly disappear from their cytoplasm. Evolution from prey to symbiont in this case can occur through cellular events repressing expulsion.

We further observed that the rate of prey phagocytosis decreases in hypoxia (Fig 6A and B) while that the cytoplasmic transit time increases. We did not observe exocytosis of *C. variabilis* in more than 8 h (Fig. 6B). Similarly, In *T. pyriformis* hypoxia induces a generalized slowdown in metabolism, including of the rate of phagocytosis (Skriver et Nilsson, 1978). Thus, by extending the prey retention time, hypoxia indirectly increases the benefit over time of oxygen intracellularly released by photosynthesis. Through genetic assimilation or accommodation (Braendle et Flatt, 2006; Kelly, 2019; Schneider et Meyer, 2017), these phenotypic changes in response to oxygen deficiency could promote genetic adaptation leading to photosynthetic endosymbiosis. Ecological observations further support that photosymbiosis occurs in hypoxia. In a stratified freshwater pond, 96% of ciliated protozoa living at the below the oxic-anoxic limit were found to host algae (Finlay et al., 1996). Oxygen produced by photosynthetic

Symbiodiniaceae was also suggested to improve survival of *Anthopleura elegantissima* and *Anemonia viridis* hosts in hypoxic environments (Malcolm et Brown, 1977; Rands et al., 1992). In aquatic environment, protozoa predators like ciliates are abundant and compete for feeding on large numbers of other microorganisms (Aijaz et Koudelka, 2017). The intracellular presence of phagocyted photosynthetic preys, even transiently, can provide an extended phenotype allowing expansion of the ecological niche into hypoxic hunting zones, and possible refuge from competitors and predators (Finlay et al., 1996; Gavelis et Gile, 2018; Quevarec et al., 2024).

Even in long evolved photosymbiotic organisms living in normoxic atmosphere, such as algae, mitochondria are able to use directly the photosynthetically evolved oxygen (Lavergne, 1989). Plants exposed to hypoxic stress by flooding also survive better in the light than in the dark suggesting a protective role of photosynthetic oxygen (León et al., 2021; Mommer et Visser, 2005).

Dioxygen can diffuse freely across membranes and is readily useable for respiration while photosynthetic sugars require dedicated transporters to cross symbiont and host membranes and appropriate metabolic enzymes (Cenci et al., 2017). This makes O_2 a more parsimonious driving force to stabilize early events leading to photosymbiosis, sugar supply probably resulting from further molecular and cellular exaptations (Gould et Vrba, 1982). Hypoxic environments are very common, can occur transiently, and were probably prevalent during a large part of life history. Indeed, while oxygenic photosynthesis evolved at least 3 Byr ago, it took around 1.6 Byr before the apparition primary endosymbiosis at a time when oxygen was still scarce and its concentration highly variable, but where the terminal oxygen reductases that enable oxygen utilization already existed for a long time in prokaryotes (at least 3 Byr ago) and then eukaryotes via the mitochondria (2.2 Byr ago) (Degli Esposti et al., 2019; Falconet, 2012; Jabłońska et Tawfik, 2021).

Material and methods

Organisms and population maintenance

The experiments were carried out with the *T. thermophila* strain CU 427 (Fig. 1A), obtained from Dr Mochizuki (CNRS – IGH, Montpellier). The ciliate *T. thermophila* is a strictly aerobic, mobile unicellular organism with an oral apparatus and a cytoproct for phagocytosis of prey and elimination of phagocytosis waste, respectively. As is able to grow by osmotrophy *T. thermophila* were routinely cultured in Neff medium (0.5% glucose, 0.25% peptone, 0.25% yeast extract and 33.3 µM $FeCl_3$) (D. M. Cassidy-Hanley, 2012) at 30°C with shaking. *S. elongatus* UTEX 2973 was routinely cultured in BG11 medium (Stanier et al., 1979) at 28°C in light (30 µEinstein.m^{-2}.s^{-1}) with shaking. *C. variabilis* NC64A was cultured in TAP medium (Gorman et Levine, 1965) at 28°C in light (30 µEinstein.m^{-2}.s^{-1}) with shaking. TAP medium is supplemented with 700 µg. mL^{-1} ampicillin and 200 µg.mL^{-1} cefotaxime (Mustapa et al. 2016). *E. coli* strain MG1655 sod::gfp with the *sod* gene interrupted by the *gfp* gene was grown in LB media.

Microscopy and video-microscopy (Fig. 1) was performed using an inverted Nikon Eclipse Ti microscope and a Motic B3 Professional microscope supplemented with a Moticam 4000 camera.

Growth of *Tetrahymena thermophila*

For each species, we performed a standard curve to estimate the number of individuals as a function of the optical density (O.D.) measured with the Cell density meter model 40 (Fisher Scientific) (λ = 600 nm) (Fig. S1). The number of individuals was estimated using a Malassez counting chamber under microscopy.

Co-cultures of *T. thermophila* with preys *(S. elongatus, C. variabilis* or *E. coli)* was performed in rich Neff medium, in modified PP medium (33.3 µM $FeCl_3$, 0.25% proteose peptone) (D. M. Cassidy-Hanley, 2012) allowing very low growth or in minimum TAP medium (Gorman et Levine, 1965). The 'Carbon' experiments were carried out in Hungate tubes at 30°C with shaking in the dark or in the light (150 µEinstein.m^{-2}.s^{-1}) (Fig. 4). To test the advantage provided by oxygen from phagocytosed phototrophs, we co-cultured *T. thermophila* in Neff medium at 30°C under shaking with the different preys *(S. elongatus, C. variabilis* or *E. coli)* with oxygen or in anoxic Hungate tubes in the dark or in the light (150 µEinstein.m^{-2}.s^{-1}) (Fig. 5B – D). Growth in low oxygen media was maintained by a massic gas mixer Pegas 4000 MF (Columbus Instruments) with a flux of 25 ml.min^{-1} using a mix of pure N_2 and synthetic air (20% O_2 and 80% N_2). Concentration of O_2 in the continuously flushed Hungate tubes was measured with a Mettler-Toledo M700 recorder equipped with an O_2 module ppb 4700 and a nanomolar range sensitive Inpro 6900 O_2 probe calibrated with two points 0 and saturated air (237µM O_2 dissolved at 30°C). All cultures are in axenic conditions in Neff medium (Fig. 5A).

Oxygen production and consumption by the different species

O_2 consumption and production activities were measured polarographically with a Clark-type electrode in a stirred volume of 1.8 ml of corresponding medium saturated with air (237 µM O_2 at 30 °C) (Fig. S5). Activities are expressed in nmol O_2.min^{-1}.mg^{-1} proteins (Fig. 7) (proteins content from whole cells were measured with Bradford solution + 0.1M NaOH using BSA as standard) or in 10^{-16} mol O_2.min^{-1}.$cell^{-1}$ (Table 1) using standard curves (Fig. S1). Samples containing phototrophs were illuminated at light intensity of about 100 µEinstein.m^{-2}.s^{-1}. All experiments were carried out at 30°C.

Flow cytometry – phagocytosis dynamics

We measured the predation level of *T. thermophila* on the prey *S. elongatus*, *C. variabilis* or *E. coli* - GFP using flow cytometry with the measure of internal fluorescence accumulation in *T. thermophila* over time (Fig. 2, 3, 6, S2, S3 and S4). Thanks to the red autofluorescence of the phototrophs due to their photosynthetic pigments (Fig. 1F), we were able to follow timely and quantitatively the phagocytosis process using flow cytometry knowing the level of fluorescence of the free partners. In addition, after exocytosis by cytoproct, we were also able to determine the number of preys in each dropping over time, as fluorescence is still present. For flow cytometry, the scatter density plots obtained (small-angle scattering FSC versus wide angle scattering SSC signals) were gated on the population of interest, filtered to remove multiple events and then analysed for the autofluorescence intensity of the phototrophs (filter 655/LP) or the GFP fluorescence (filter 525/30) of *E. coli* strain MG1655 sod::gfp. Samples were run in the low-pressure mode and a total number of 300-500K events were collected per sample. Data were acquired with a S3e cells sorter (Bio-rad) using 488 and 561 nm lasers and were analysed and plotted using FlowJo v10.6.

Statistical analysis

Before the analysis, we square root-transformed data of O.D. or number of *T. thermophila*/µl for the growth curves in order to test the lower limit of oxygen concentration to allow growth or carbon benefit, except for the *T. thermophila – E. coli* and *T. thermophila – S. elongatus* in modified PP medium experiments, where we used raw data, not transformed. We used a Generalized Additive Mixed Model (GAMM) with R software (R Core Team, 2013) and the Mgcv package (Wood et al., 2016) to analyze and compare the curves of several experiments with gaussian distribution. No overdispersion of the data was observed. We analyzed the number of *T. thermophila* as a function of time (in hours) (a continuous variable), culture conditions (i.e., medium, prey, presence of oxygen) as fixed effects. ID of the replicate were

added as random effects. The smoothing was performed on the variable time in function of culture condition. A contrast matrix is created for pairwise comparison of each culture condition with glht function of multcomp package (Hothorn et al., 2008) for ‘carbon’ experiments with at least 4 different treatments (Table S1C and S2C). We used Kruskal-Wallis rank sum test with R software and the stats package (R Core Team, 2013) to compare the growth of *T. thermophila* in anoxia with phototrophs (*S. elongatus, C. variabilis*) or *E. coli* in light and dark. Then, a post hoc pairwise comparison (Dunn’s test) with Holm correction was realized between each treatment with rstatix package (Kassambara, 2019).

Acknowledgments

We thank Dr. K. Mochizuki, T. Noto and J. Saksouk (IGH CNRS Montpellier, France), Aaron P. Turkewitz (Chicago University, U.S.A.) for the kind gift of *Tetrahymena thermophila* strains and precious advices. We thank the Cyanobacteria team at LCB-Marseille (Prof. A. Latifi, V. Risoul, A. Scholivet, S. Champ) for the kind gift of *Synechococcus elongatus* and the use of equipments, Dr. B. Ezraty and Prof. L. Aussel for *E. coli* strains, and Dr. Y. Li-Beisson and P. Auroy-Tarrago (BIAM) for *Chlorella variabilis*. We also thank Prof. D. Aragnol and S. Ridaoui (master student) for preliminary experiments, we thank the students V. Faroux and Y. Allio for their help with some experiments. Our IAM team is also acknowledged for support and Dr. L. Espinosa for microscopy advices. We thank P. Notareschi and A. Grossi for 3D printing accessories. This project PHOCEE N° 21-CE20-0035 to CR and GB was financially supported by the ANR agency and by IM2B (Institut de Microbiologie, Bioénergies et Biotechnologie, Aix-Marseille University) for a fellowship to RB.

Conflict of interest

The authors declare no conflict of interest.

Author contributions

LQ, CR and GB conceptualized the study. LQ, RB, CR and GB designed the experiments. LQ, RB and GB performed the experiments and collected the data. LQ and GB performed the statistical analysis. LQ, CR and GB wrote the manuscript. All authors read, comment and approved the final manuscript.

References

Adomako, M., Ernst, D., Simkovsky, R., Chao, Y.-Y., Wang, J., Fang, M., Bouchier, C., Lopez-Igual, R., Mazel, D., Gugger, M. et Golden, S. S. (2022). Comparative Genomics of Synechococcus elongatus Explains the Phenotypic Diversity of the Strains. *MBio*, *13*(3), e00862-22. https://doi.org/10.1128/mbio.00862-22

Aijaz, I. et Koudelka, G. B. (2017). Tetrahymena phagocytic vesicles as ecological micro-niches of phage transfer. *FEMS Microbiology Ecology*, *93*(4). https://doi.org/10.1093/femsec/fix030

Apple, J. K., Strom, S. L., Palenik, B. et Brahamsha, B. (2011). Variability in Protist Grazing and Growth on Different Marine Synechococcus Isolates. *Applied and Environmental Microbiology*, *77*(9), 3074-3084. https://doi.org/10.1128/AEM.02241-10

Archibald, J. M. (2015). Endosymbiosis and Eukaryotic Cell Evolution. *Current Biology*, *25*(19), R911-R921. https://doi.org/10.1016/j.cub.2015.07.055

Avila-Poveda, O. H., Torres-Ariño, A., Girón-Cruz, D. A. et Cuevas-Aguirre, A. (2014). Evidence for accumulation of Synechococcus elongatus (Cyanobacteria: Cyanophyceae) in the tissues of the oyster Crassostrea gigas (Mollusca: Bivalvia). *Tissue and Cell*, *46*(5), 379-387. https://doi.org/10.1016/j.tice.2014.07.001

Bhattacharya, D., Etten, J. V., Benites, L. F. et Stephens, T. G. (2023). Endosymbiotic ratchet accelerates divergence after organelle origin: The *Paulinella* model for plastid evolution. *BioEssays*, *45*(1), 2200165. https://doi.org/10.1002/bies.202200165

Bowles, A. M. C., Williamson, C. J., Williams, T. A., Lenton, T. M. et Donoghue, P. C. J. (2023). The origin and early evolution of plants. *Trends in Plant Science*, *28*(3), 312-329. https://doi.org/10.1016/j.tplants.2022.09.009

Braendle, C. et Flatt, T. (2006). A role for genetic accommodation in evolution? *BioEssays*, *28*(9), 868-873. https://doi.org/10.1002/bies.20456

Cassidy-Hanley, D. M. (2012). Tetrahymena in the Laboratory: Strain Resources, Methods for Culture, Maintenance, and Storage. Dans *Methods in Cell Biology* (vol. 109, p. 237-276). Elsevier. https://doi.org/10.1016/B978-0-12-385967-9.00008-6

Cavalcanti, V. L. R., Brandão-Costa, R. M. P., Pontual, E. V., de Andrade, A. F., Alves, L. C., Porto, A. L. F. et Bezerra, R. P. (2021). Chlorella vulgaris lectin kills Aedes aegypti larvae. *Algal Research*, *56*, 102290. https://doi.org/10.1016/j.algal.2021.102290

Cenci, U., Bhattacharya, D., Weber, A. P. M., Colleoni, C., Subtil, A. et Ball, S. G. (2017). Biotic Host–Pathogen Interactions As Major Drivers of Plastid Endosymbiosis. *Trends in Plant Science*, *22*(4), 316-328. https://doi.org/10.1016/j.tplants.2016.12.007

Christaki, U., Jacquet, S., Dolan, J. R., Vaulot, D. et Rassoulzadegan, F. (1999). Growth and grazing on Prochlorococcus and Synechococcus by two marine ciliates. *Limnology and Oceanography*, *44*(1), 52-61. https://doi.org/10.4319/lo.1999.44.1.0052

Degli Esposti, M., Mentel, M., Martin, W. et Sousa, F. L. (2019). Oxygen Reductases in Alphaproteobacterial Genomes: Physiological Evolution From Low to High Oxygen Environments. *Frontiers in Microbiology*, *10*, 499. https://doi.org/10.3389/fmicb.2019.00499

Delaye, L., Valadez-Cano, C. et Pérez-Zamorano, B. (2016). How Really Ancient Is Paulinella Chromatophora? *PLoS Currents*. https://doi.org/10.1371/currents.tol.e68a099364bb1a1e129a17b4e06b0c6b

Dillon, A. et Parry, J. D. (2009). Amoebic grazing of freshwater Synechococcus strains rich in phycocyanin: Amoebic grazing of freshwater Synechococcus spp. *FEMS Microbiology Ecology*, *69*(1), 106-112. https://doi.org/10.1111/j.1574-6941.2009.00690.x

Dolan, J. R. et Šimek, K. (1998). Ingestion and digestion of an autotrophic picoplankter, Synechococcus, by a heterotrophic nanoflagellate, Bode saLtans. *Limnology and Oceanography*, *43*(7), 1740-1746. https://doi.org/10.4319/lo.1998.43.7.1740

Falconet, D. (2012). Origin, Evolution and Division of Plastids. Dans J. J. Eaton-Rye, B. C. Tripathy et T. D. Sharkey (dir.), *Photosynthesis* (vol. 34, p. 35-61). Springer Netherlands. https://doi.org/10.1007/978-94-007-1579-0_2

Finlay, B. J., Maberly, S. C. et Esteban, G. F. (1996). Spectacular abundance of ciliates in anoxic pond water: contribution of symbiont photosynthesis to host respiratory oxygen requirements. *FEMS Microbiology Ecology*, *20*(4), 229-235. https://doi.org/10.1111/j.1574-6941.1996.tb00321.x

Fischer, W. W., Hemp, J. et Johnson, J. E. (2016). Evolution of Oxygenic Photosynthesis. *Annual Review of Earth and Planetary Sciences*, *44*(1), 647-683. https://doi.org/10.1146/annurev-earth-060313-054810

Fujishima, M. et Kodama, Y. (2022). Mechanisms for establishing primary and secondary endosymbiosis in *Paramecium*. *Journal of Eukaryotic Microbiology*, *69*(5), e12901. https://doi.org/10.1111/jeu.12901

Gavelis, G. S. et Gile, G. H. (2018). How did cyanobacteria first embark on the path to becoming plastids?: lessons from protist symbioses. *FEMS Microbiology Letters*, *365*(19). https://doi.org/10.1093/femsle/fny209

Germond, A., Kunihiro, T., Inouhe, M. et Nakajima, T. (2013). Physiological changes of a green alga (Micractinium sp.) involved in an early-stage of association with Tetrahymena thermophila during 5-year microcosm culture. *Biosystems*, *114*(3), 164-171. https://doi.org/10.1016/j.biosystems.2013.08.005

Gorman, D. S. et Levine, R. P. (1965). Cytochrome f and plastocyanin: their sequence in the photosynthetic electron transport chain of Chlamydomonas reinhardi. *Proceedings of*

the National Academy of Sciences, *54*(6), 1665-1669. https://doi.org/10.1073/pnas.54.6.1665

Gould, S. J. et Vrba, E. S. (1982). Exaptation—a Missing Term in the Science of Form. *Paleobiology*, *8*(1), 4-15. https://doi.org/10.1017/S0094837300004310

Gurijala, K. R. et Alexander, M. (1990). Effect of growth rate and hydrophobicity on bacteria surviving protozoan grazing. *Applied and Environmental Microbiology*, *56*(6), 1631-1635. https://doi.org/10.1128/aem.56.6.1631-1635.1990

Hoefnagel, M. H., Atkin, O. K. et Wiskich, J. T. (1998). Interdependence between chloroplasts and mitochondria in the light and the dark. *Biochimica et Biophysica Acta (BBA)-Bioenergetics*, *1366*(3), 235-255.

Hoshina, R., Tsukii, Y., Harumoto, T. et Suzaki, T. (2021). Characterization of a green Stentor with symbiotic algae growing in an extremely oligotrophic environment and storing large amounts of starch granules in its cytoplasm. *Scientific Reports*, *11*(1), 2865. https://doi.org/10.1038/s41598-021-82416-9

Hothorn, T., Bretz, F. et Westfall, P. (2008). Simultaneous Inference in General Parametric Models. *Biometrical Journal*, *50*(3), 346-363. https://doi.org/10.1002/bimj.200810425

Inouye, I. et Okamoto, N. (2005). Changing concepts of a plant: current knowledge on plant diversity and evolution. *Plant Biotechnology*, *22*(5), 505-514. https://doi.org/10.5511/plantbiotechnology.22.505

Jabłońska, J. et Tawfik, D. S. (2021). The evolution of oxygen-utilizing enzymes suggests early biosphere oxygenation. *Nature Ecology & Evolution*, *5*(4), 442-448. https://doi.org/10.1038/s41559-020-01386-9

Johnson, M. D. (2011). The acquisition of phototrophy: adaptive strategies of hosting endosymbionts and organelles. *Photosynthesis Research*, *107*(1), 117-132. https://doi.org/10.1007/s11120-010-9546-8

Karakashian, S. J. et Rudzinska, M. A. (1981). Inhibition of lysosomal fusion with symbiont-containing vacuoles in Paramecium bursaria. *Experimental Cell Research*, *131*(2), 387-393. https://doi.org/10.1016/0014-4827(81)90242-1

Kassambara, A. (2019). rstatix: Pipe-friendly framework for basic statistical tests. *CRAN: Contributed Packages*.

Keeling, P. J. (2010). The endosymbiotic origin, diversification and fate of plastids. *Philosophical Transactions of the Royal Society B: Biological Sciences*, *365*(1541), 729-748. https://doi.org/10.1098/rstb.2009.0103

Kelly, M. (2019). Adaptation to climate change through genetic accommodation and assimilation of plastic phenotypes. *Philosophical Transactions of the Royal Society B: Biological Sciences*, *374*(1768), 20180176. https://doi.org/10.1098/rstb.2018.0176

Kodama, Y., Nakahara, M. et Fujishima, M. (2007). Symbiotic alga Chlorella vulgaris of the ciliate Paramecium bursaria shows temporary resistance to host lysosomal enzymes during the early infection process. *Protoplasma*, *230*(1-2), 61-67. https://doi.org/10.1007/s00709-006-0193-z

Kodama, Y. et Sumita, H. (2022). The ciliate Paramecium bursaria allows budding of symbiotic Chlorella variabilis cells singly from the digestive vacuole membrane into the cytoplasm during algal reinfection. *Protoplasma*, *259*(1), 117-125. https://doi.org/10.1007/s00709-021-01645-x

Krienitz, L., Huss, V. A. R. et Bock, C. (2015). Chlorella: 125 years of the green survivalist. *Trends in Plant Science*, *20*(2), 67-69. https://doi.org/10.1016/j.tplants.2014.11.005

Lane, C. E. et Archibald, J. M. (2008). The eukaryotic tree of life: endosymbiosis takes its TOL. *Trends in Ecology & Evolution*, *23*(5), 268-275. https://doi.org/10.1016/j.tree.2008.02.004

Lavergne, J. (1989). Mitochondrial responses to intracellular pulses of photosynthetic oxygen. *Proceedings of the National Academy of Sciences*, *86*(22), 8768-8772. https://doi.org/10.1073/pnas.86.22.8768

León, J., Castillo, M. C. et Gayubas, B. (2021). The hypoxia–reoxygenation stress in plants. *Journal of Experimental Botany*, *72*(16), 5841-5856. https://doi.org/10.1093/jxb/eraa591

Lürling, M. (2021). Grazing resistance in phytoplankton. *Hydrobiologia*, *848*(1), 237-249. https://doi.org/10.1007/s10750-020-04370-3

Lynn, D. H. et Doerder, F. P. (2012). The Life and Times of Tetrahymena. Dans *Methods in Cell Biology* (vol. 109, p. 9-27). Elsevier. https://doi.org/10.1016/B978-0-12-385967-9.00002-5

Malcolm, J. M. et Brown, W. I. (1977). Zooxanthellae-produced O2 promotes sea anemone expansion and eliminates oxygen debt under environmental hypoxia. *Journal of Experimental Zoology*, *201*(1), 149-155. https://doi.org/10.1002/jez.1402010118

Matsui, K., Kono, S., Saeki, A., Ishii, N., Min, M.-G. et Kawabata, Z. ichiro. (2000). Direct and indirect interactions for coexistence in a species-defined microcosm. *Hydrobiologia*, *435*, 109-116.

Matzke, B., Schwarzmeier, E. et Loos, E. (1990). Maltose excretion by the symbiotic Chlorella of the heliozoan Acanthocystis turfacea. *Planta*, *181*(4). https://doi.org/10.1007/BF00193015

Mommer, L. et Visser, E. J. W. (2005). Underwater Photosynthesis in Flooded Terrestrial Plants: A Matter of Leaf Plasticity. *Annals of Botany*, *96*(4), 581-589. https://doi.org/10.1093/aob/mci212

Mustapa, M., Sallehudin, N. J., Mohamed, M. S., Noor, N. M. et Raus, R. A. (2016). Decontamination of Chlorella sp. culture using antibiotics and antifungal cocktail treatment. *ARPN J. Eng. Appl. Sci*, *11*, 104-109.

Nowack, E. C. M., Melkonian, M. et Glöckner, G. (2008). Chromatophore Genome Sequence of Paulinella Sheds Light on Acquisition of Photosynthesis by Eukaryotes. *Current Biology*, *18*(6), 410-418. https://doi.org/10.1016/j.cub.2008.02.051

Pitsch, G., Adamec, L., Dirren, S., Nitsche, F., Šimek, K., Sirová, D. et Posch, T. (2017). The Green *Tetrahymena utriculariae* n. sp. (Ciliophora, Oligohymenophorea) with Its Endosymbiotic Algae (*Micractinium* sp.), Living in Traps of a Carnivorous Aquatic Plant. *Journal of Eukaryotic Microbiology*, *64*(3), 322-335. https://doi.org/10.1111/jeu.12369

Ponce-Toledo, R. I., López-García, P. et Moreira, D. (2019). Horizontal and endosymbiotic gene transfer in early plastid evolution. *New Phytologist*, *224*(2), 618-624. https://doi.org/10.1111/nph.15965

Quevarec, L., Brasseur, G., Aragnol, D. et Robaglia, C. (2024). Tracking the early events of photosymbiosis evolution. *Trends in Plant Science*, *29*(4), 406-412. https://doi.org/10.1016/j.tplants.2023.11.005

R Core Team. (2013). R: A language and environment for statistical computing. *Foundation for Statistical Computing, Vienna, Austria*.

Rajević, N., Kovačević, G., Kalafatić, M., Gould, S. B., Martin, W. F. et Franjević, D. (2015). Algal endosymbionts in European Hydra strains reflect multiple origins of the zoochlorella symbiosis. *Molecular Phylogenetics and Evolution*, *93*, 55-62. https://doi.org/10.1016/j.ympev.2015.07.014

Rands, M. L., Douglas, A. E., Loughman, B. C. et Ratcliffe, R. G. (1992). Avoidance of Hypoxia in a Cnidarian Symbiosis by Algal Photosynthetic Oxygen. *The Biological Bulletin*, *182*(1), 159-162. https://doi.org/10.2307/1542191

Sano, A., Watanabe, M. et Nakajima, T. (2009). Adaptive characteristics of a ciliateTetrahymena thermophila in endosymbiotic association with a green algaChlorella vulgaris derived in a long-term microcosm culture. *Symbiosis*, *47*(3), 151-160. https://doi.org/10.1007/BF03179975

Schneider, R. F. et Meyer, A. (2017). How plasticity, genetic assimilation and cryptic genetic variation may contribute to adaptive radiations. *Molecular Ecology*, *26*(1), 330-350. https://doi.org/10.1111/mec.13880

Skriver, L. et Nilsson, J. R. (1978). The Relationship between Energy-dependent Phagocytosis and the Rate of Oxygen Consumption in Tetrahymena. *Journal of General Microbiology*, *109*(2), 359-366. https://doi.org/10.1099/00221287-109-2-359

Stanier, R. Y., Deruelles, J., Rippka, R., Herdman, M. et Waterbury, J. B. (1979). Generic Assignments, Strain Histories and Properties of Pure Cultures of Cyanobacteria. *Microbiology*, *111*(1), 1-61. https://doi.org/10.1099/00221287-111-1-1

Wloga, D. et Frankel, J. (2012). From Molecules to Morphology: Cellular Organization of Tetrahymena thermophila. Dans *Methods in Cell Biology* (vol. 109, p. 83-140). Elsevier. https://doi.org/10.1016/B978-0-12-385967-9.00005-0

Wood, S. N., Pya, N. et Säfken, B. (2016). Smoothing Parameter and Model Selection for General Smooth Models. *Journal of the American Statistical Association*, *111*(516), 1548-1563. https://doi.org/10.1080/01621459.2016.1180986

Zagata, P., Greczek-Stachura, M., Tarcz, S. et Rautian, M. (2016). The Evolutionary Relationships between Endosymbiotic Green Algae of <I>Paramecium bursaria</I>

Syngens Originating from Different Geographical Locations. *Folia Biologica*, *64*(1), 47-54. https://doi.org/10.3409/fb64_1.47

Tables and figures

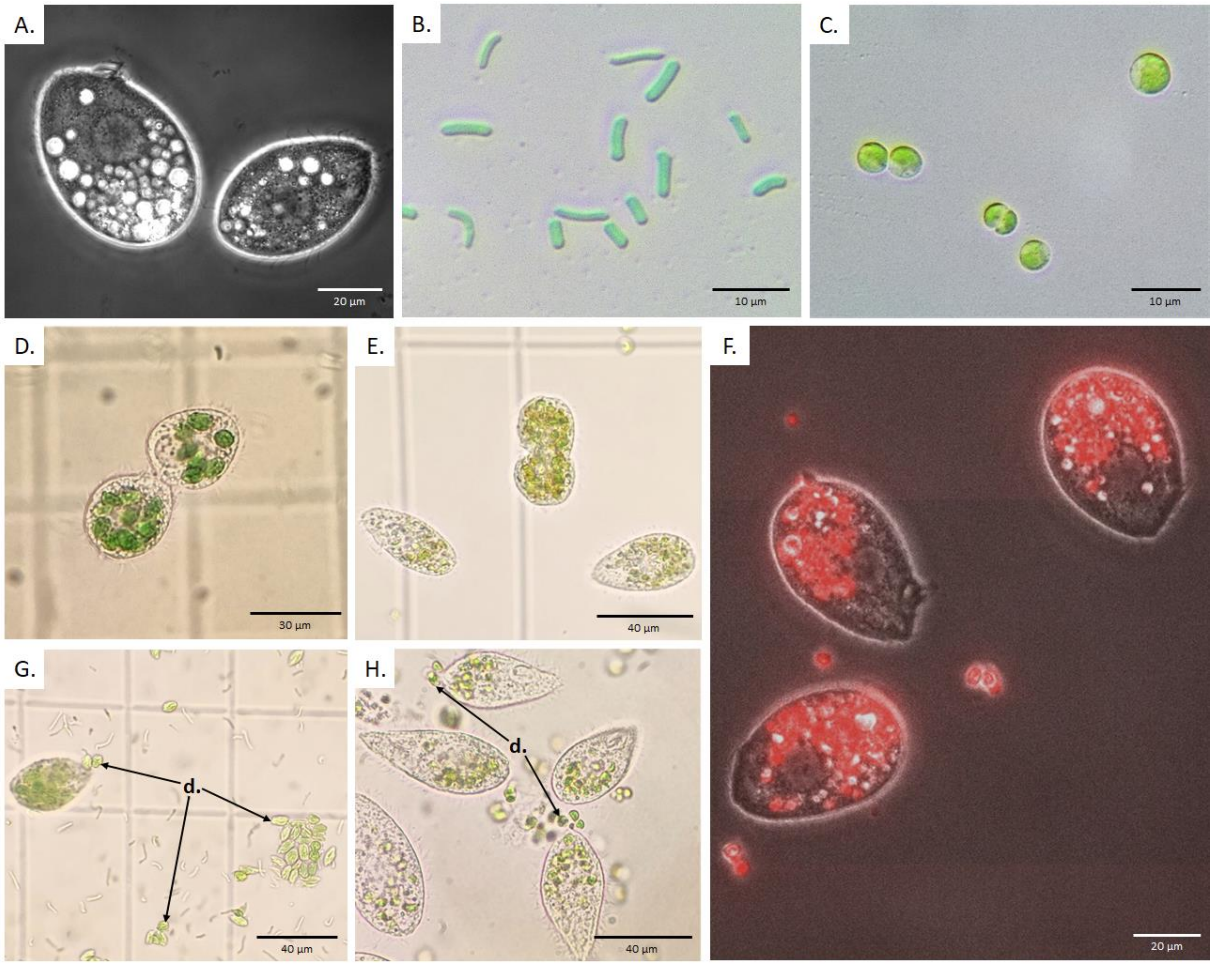

Figure 1: optical microscopy representing **A.** *T. thermophila*, **B.** *S. elongatus* and **C.** *C. variabilis* cells. **D.** and **E.** *S. elongatus* and *C. variabilis* in *T. thermophila* cells undergoing mitosis, respectively. **F.** *C. variabilis* phagocytosed by *T. thermophila* under fluorescence. **G.** and **H.** Green droppings (**d.**) exocytosed by *T. thermophila* and containing *S. elongatus* and *C. variabilis* cells, respectively.

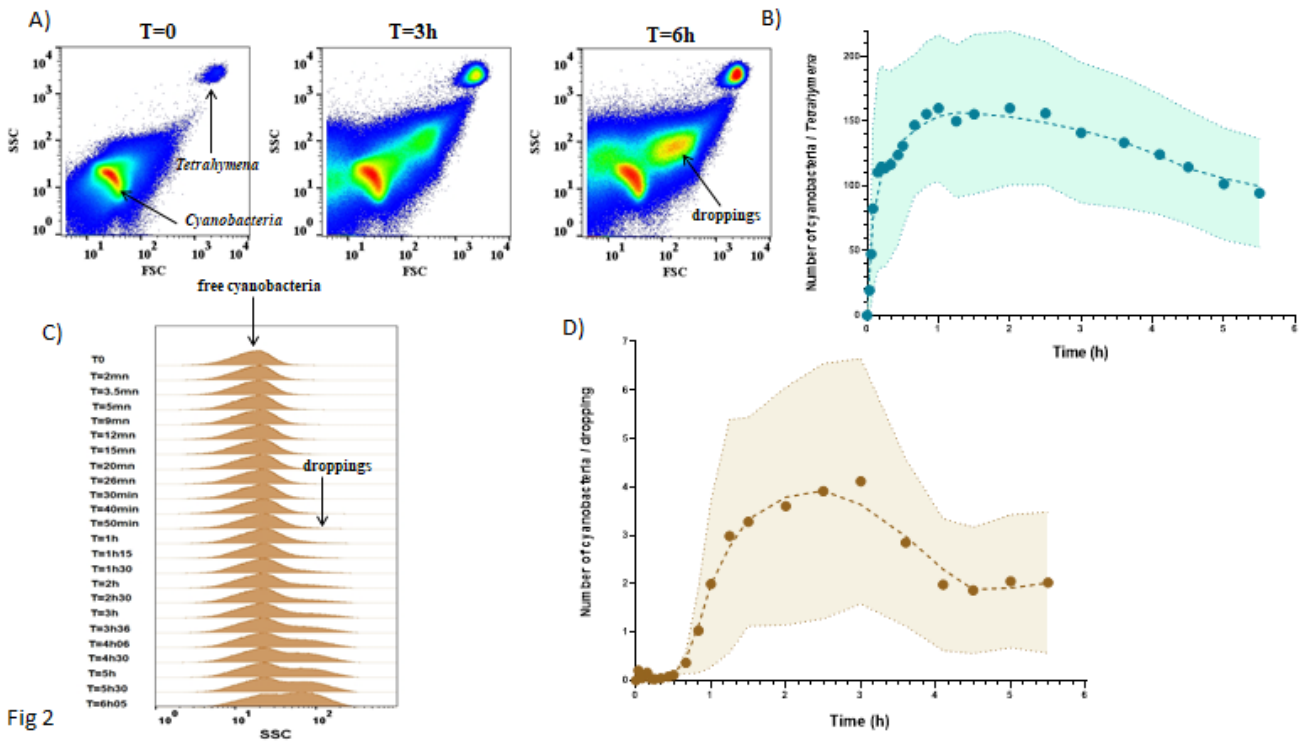

Fig 2

Figure 2: phagocytosis of cyanobacteria *S. elongatus* (SE) by the ciliate *T. thermophila* (TT) **A)** Analysis of populations of cyanobacteria SE mixed with TT in oxic conditions at 30°C (initial ratio of 400 SE/TT). The apparition of TT droppings composed of fluorescent SE is indicated. Color code from blue to red indicates low to high relative density of populations respectively, in a constant number of total events per point (n = 8 x10^5). **B)** Kinetics SE transit inside of TT using the intrinsic red autofluorescence of SE. Shaded area corresponds to the standard deviation of fluorescence mean. **C)** SSC scatter histograms of free cyanobacteria SE and the new population corresponding to the formation of droppings (see Fig. 2A). **D)** Kinetics of droppings formation expressed as the number of SE per dropping as a function of time.

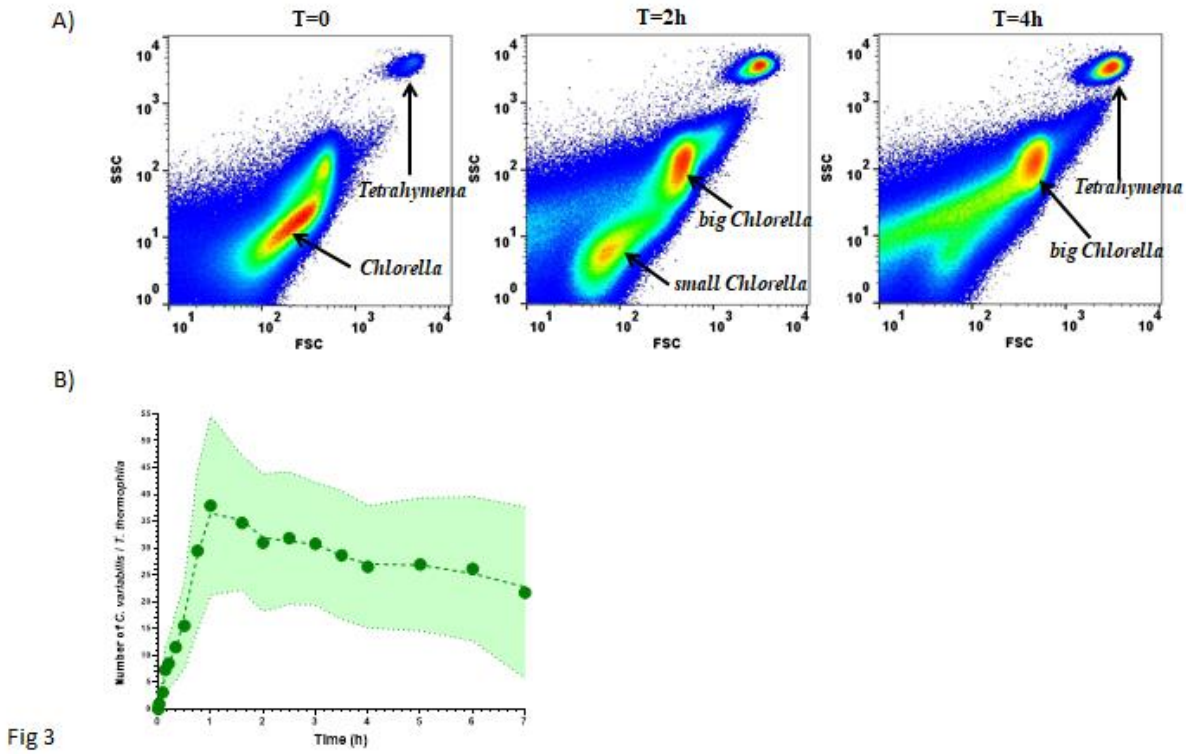

Fig 3

Figure 3: phagocytosis of *C. variabilis* (CV) by *T. thermophila* (TT). **A)** Analysis of populations of Chlorella mixed with TT in oxic conditions at 30°C (initial ratio of 200 CV/TT). Flow cytometry scatter density plots (SSC versus FSC) shows the larger size of TT, the smaller diffraction of the CV and the disappearing of smaller CV as a function of time. Color code from blue to red indicates low to high relative density of populations respectively, in a constant number of total events per point (n = 8 x 10^5). **B)** Kinetics of the transit time of CV phagocyted per TT using the intrinsic red autofluorescence of CV. Shaded area corresponds to the standard deviation of fluorescence mean.

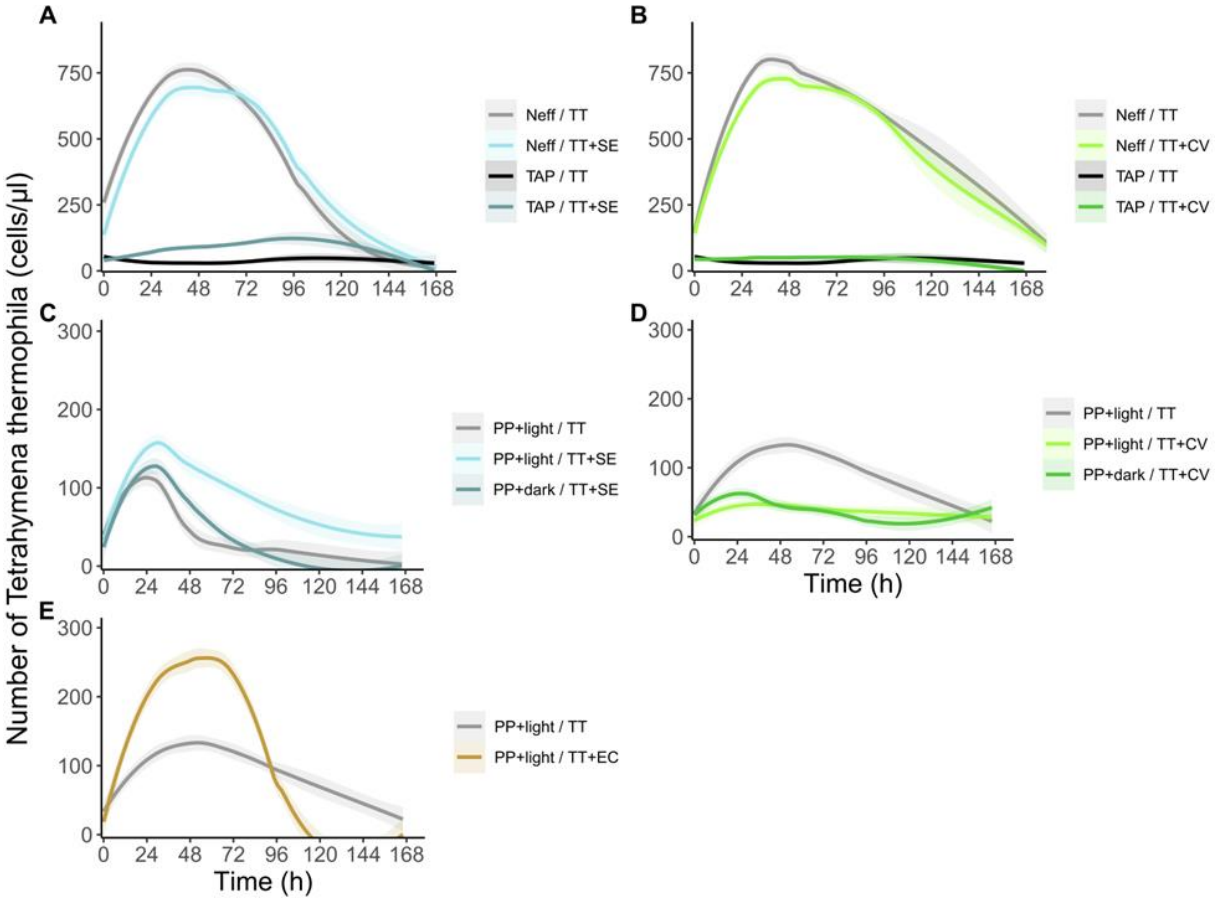

Figure 4: contribution of prey microorganisms as carbon sources to *T. thermophila* (TT) growth. Shaded areas represent 95% confidence intervals. **A.** and **B.** Growth of *T. thermophila* in a rich Neff medium and mineral minimum TAP medium with **A.** *S. elongatus* (SE) or **B.** *C. variabilis* (CV); **C.** and **D.** Growth in modified PP medium in light or dark with **C.** *S. elongatus* (SE) or **D.** *C. variabilis* (CV); **E.** Growth in modified PP medium with *E. coli* (EC). The data were analyzed using GAMM. All the results of the statistical test are shown in Table S1 - S5. Briefly, we observed a significant growth of *T. thermophila* in the rich Neff medium with SE (**A.** p-value < 0.001***) or CV (**B.** p-value < 10^{-6}***) or without phototrophs (**A.** p-value < 0.001*** and **B.** p-value < 10^{-6}***) compared with a culture TAP medium. In TAP medium, only SE increased slightly the growth of TT (**A.** p-value < 0.001***). In the modified PP medium, **C.** SE stimulated the growth of TT in the light (p-value = 5.36 x 10^{-5}***) but not in the dark (p-value = 0.556), while **D.** CV decreased the growth of TT both in the light (p-value

= 0.000324***) and in the dark (p-value = 0.000376***). **E.** EC stimulated the growth of TT (p-value = 5.69 x 10^{-8}***). ns: no significant; *, $P < 0.05$; **, $P < 0.01$; ***, $P < 0.001$.

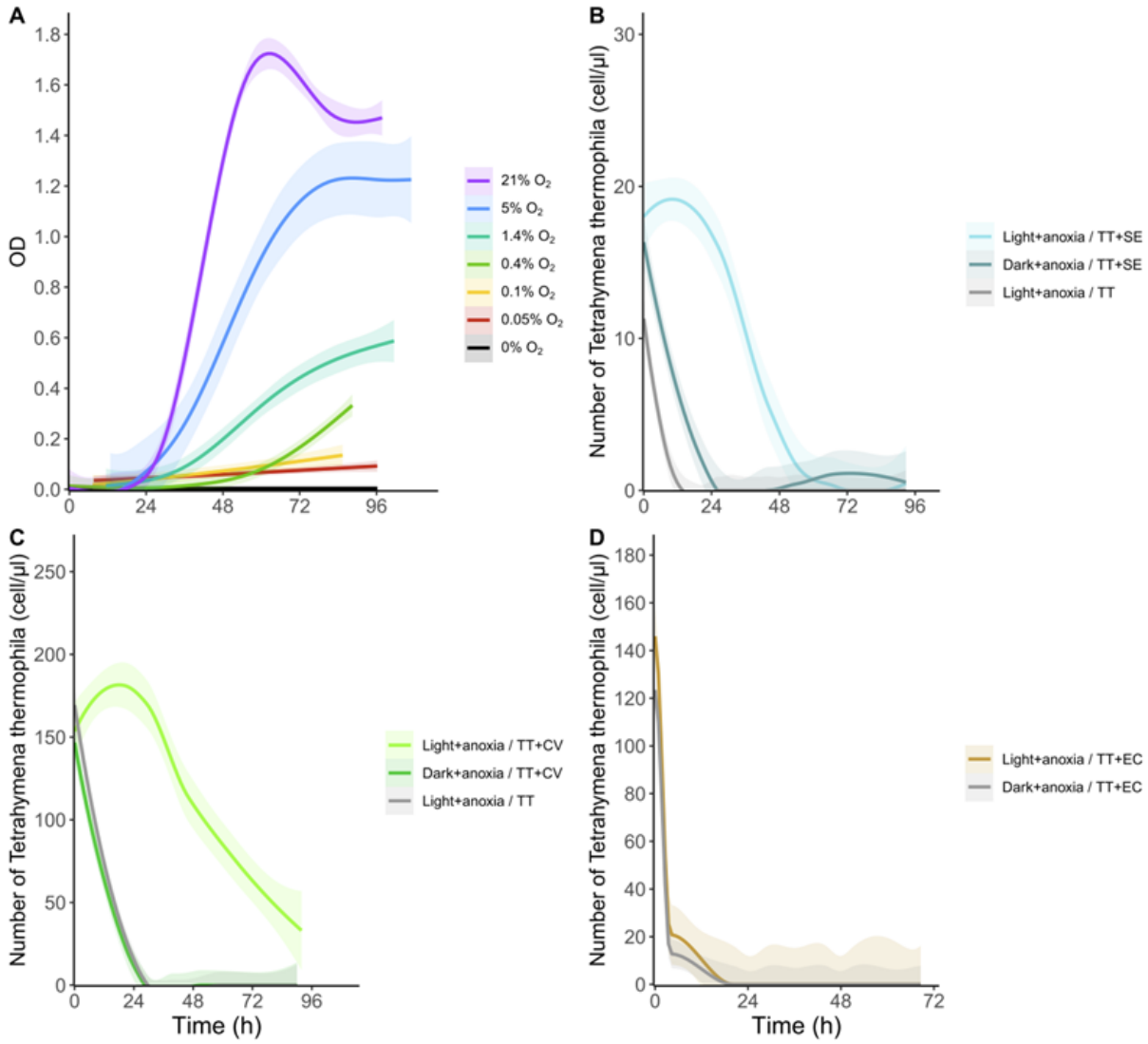

Figure 5: Contribution of prey microorganisms to *T. thermophila* (TT) growth in limiting oxygen. Shaded areas represent 95% confidence intervals. **A.** Growth of *T. thermophila* estimate by measuring the OD (λ = 600 nm) of the culture with increasing oxygen concentrations ranging from 0% (pure N_2) to atmospheric level of 21% O_2. The data were analyzed using a GAMM. Shaded areas represent 95% confidence intervals. All the results of the statistical test are shown in Table S6. Briefly, we observed a significant growth for 0.05% oxygen (p-value = 0.0138*), 0.1% (p-value = 0.0119*), 0.4% (p-value = 0.011*), 1.4% (p-value

= 5.22 x 10^{-6}***), 5% (p-value = 5.27 x 10^{-12}***), 21% (p-value < 2 x 10^{-16}***). **B.** to **D.** Growth of *T. thermophila* under anoxic conditions in light or dark, with or without prey (**B.** *S. elongatus* (SE), **C.** *C. variabilis* (CV) and **D.** *E. coli* (EC)). The data was analyzed using a Kruskal-Wallis rank sum test and a post hoc pairwise comparison (Dunn's test) with Holm correction. Results: **B.** Kruskal-Wallis chi-squared = 68.647, df = 2, p-value = 1.24 x 10^{-15}***: light alone vs light with *S. elongatus*: Dunn's test: adjusted p-value = 5.43 x 10^{-16}***, dark with *S. elongatus* vs light with *S. elongatus*: Dunn's test: adjusted p-value = 2.78 x 10^{-5}***. **C.** Kruskal-Wallis chi-squared = 106.93, df = 2, p-value < 2.2 x 10^{-16}***: light alone vs light with *C. variabilis*: Dunn's test: adjusted p-value = 4.31 x 10^{-13}***, dark with *C. variabilis* vs light with *C. variabilis*: Dunn's test: adjusted p-value = 3.29 x 10^{-20}***. **D.** dark with *E. coli* vs light with *E. coli*: Kruskal-Wallis chi-squared = 0.3375, df = 1, p-value = 0.5613***. ns: no significant; *, $P < 0.05$; **, $P < 0.01$; ***, $P < 0.001$.

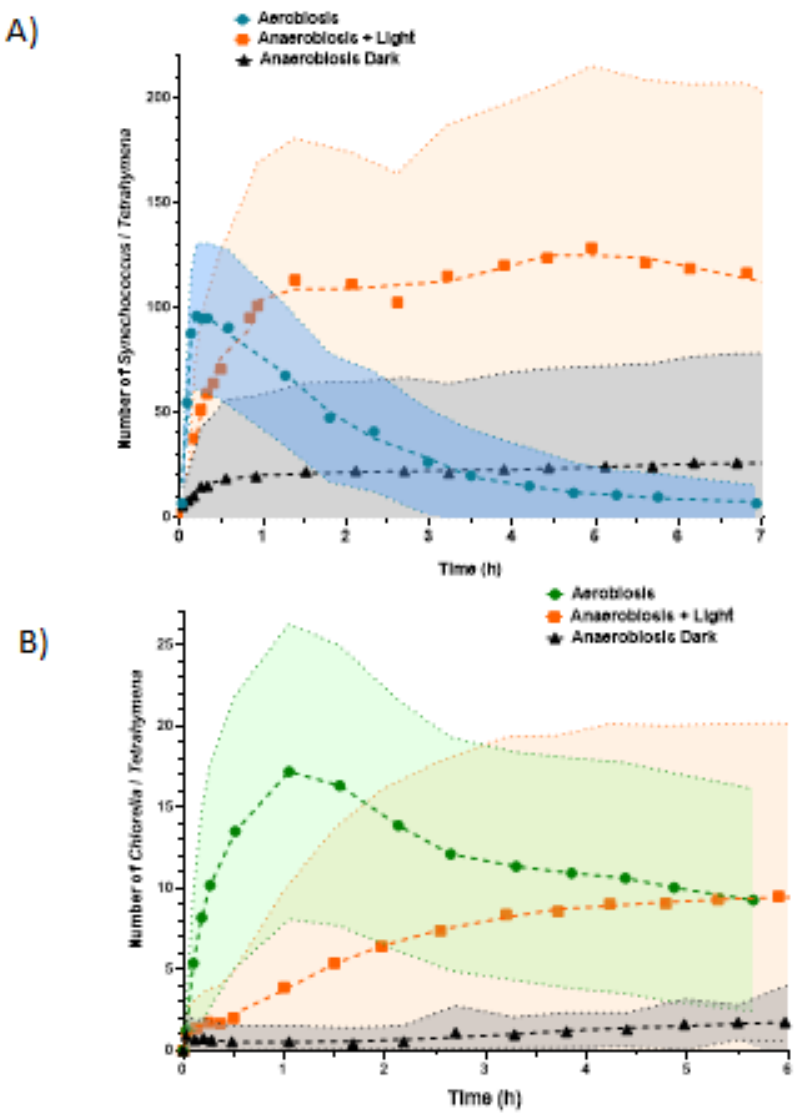

Figure 6: O_2 produced by the phototrophs allows *T. thermophila* (TT) phagocytosis in anaerobiosis. **A)** Kinetics of *S. elongatus* (SE) transit within TT in oxic condition (atmospheric 21% O_2, cyan dots), in anoxic conditions in the dark (black triangle) or in anoxic conditions in the light (orange square) at 30°C (initial ratio of 500 SE/TT). **B)** Kinetics of *C. variabilis* (CV) transit time within TT in oxic condition (atmospheric 21% O_2, green dots), in anoxic conditions in the dark (black triangle) or in anoxic conditions in the light (orange square) (initial ratio of 150 CV/TT). Shaded area corresponds to the standard deviation of fluorescence mean (cytometry total events per point: n = 10^6).

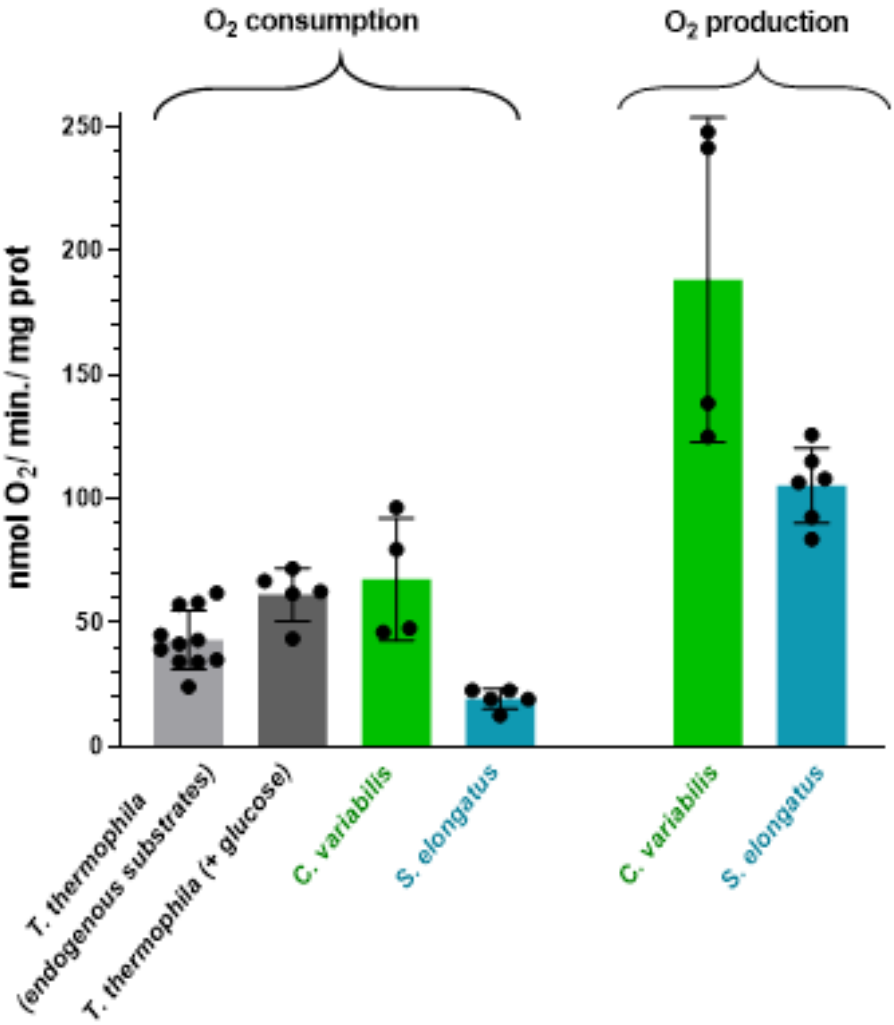

Figure 7: O_2 evolution by the photosynthetic preys cyanobacteria and chlorella is compatible with *T. thermophila* aerobic metabolism. O_2 consumption and production activities (nmol O_2/mg/min, see Fig. S5) corresponding to maximum values with endogenous substrates, in saturation of substrate (glucose 20 mM) or in presence of saturating light for the phototrophs (60-100 µmoles photons/m^2/s) are shown for the three organisms. See Table 1 for production and consumption of O_2 at the single cell level.

Table 1: O_2 evolution by the phototrophs cyanobacteria and chlorella and O_2 consumption by *T. thermophila* are compatible at the single cell level with photo-endosymbiosis. From calibration curves presented in Fig. S6, O_2 production and consumption at the cellular level for the three organisms was calculated. Results from Fig. 7 expressed per cell indicate that for maximum *T. thermophila* oxygen consumption rate, it requires the equivalent of about 260 chlorella and 1500 cyanobacteria producing O_2 by photosynthesis.

	O_2 consumption (nmol O_2/min./**cell**)	**O_2 production** (nmol O_2/min./**cell**)	***T. thermophila* O_2 consumption / phototroph O_2 production**
Tetrahymena thermophila	600×10^{-7}	n.a.	n.a.
Chlorella variabilis	0.82×10^{-7}	2.3×10^{-7}	260
Synechococcus elongatus	0.073×10^{-7}	0.40×10^{-7}	1500